CHALLENGES OF A CENTRAL OR DECENTRALIZED SOLAR SUPPLY OF SOLAR DISTRICT HEATING GRIDS

Markus Rabensteiner[a], Peter Schatte[b], Wolfgang Leitner[c] and Alois Kraußler[d]

[a] 4ward Energy Research GmbH, Headquarters, Reininghausstraße 13A, 8020 Graz, Austria, +43 (0)664 88 251 830, markus.rabensteiner@4wardenergy.at

[b] Hoval GmbH, Holzinnovationszentrum 1a, 8740 Zeltweg, Austria, +43 (0)664 600 555 311, peter.schatte@hoval.at

[c] Hoval GmbH, Holzinnovationszentrum 1a, 8740 Zeltweg, Austria, +43 (0)50 3655 341, wolfgang.leitner@hoval.at

[d] 4ward Energy Research GmbH, Site Vorau, Impulszentrum 1, 8250 Vorau, Austria, +43 (0)664 88 500 339, alois.kraussler@4wardenergy.at

Abstract – Energy management systems that guarantee a system-wide control of district heating systems are already state of the art. However, a bidirectional heat transfer station (for heat supply and uptake) in combination with an intelligent control strategy for the entire district heating system still has to be developed. While in a laboratory test, the properties of a prosumer are examined, a numerical model is used to investigate the effects of several prosumer on the entire district heating system. The simulation model, consisting of two parts, allows to investigate the bidirectional heat transfer station. The first model part depicts the primary side of the district heating system. Data from a real-life medium-sized district heating system is used as reference. The second part of the model forms the bidirectional heat transfer station and is individually set for each prosumer. A secondary storage exchanges energy with the decentralized heat source, the district heating system and the heating system of the consumer. The numerical model allows an energetic and economic investigation of district heating systems containing several prosumers. Hydraulic problems such as flow reversals can also be investigated. The simulation model has been validated on the basis of laboratory experiments.

1. INTRODUCTION

Local and district heating is an environmentally friendly heat supply by efficient energy generation plants, the use of combined heat and power and the use of residual and waste heat. About 24 % of all apartments in Austria are heated with local or district heating (FGW, 2016). However, operators (especially of smaller and medium-sized grids) are faced with economic challenges concerning decreasing heat demand due to better building standards (Averfalk and Werner, 2017; Lund et al., 2010). The exploitation of all optimization potentials by means of efficiency improvement measures (heating plant, grid and consumer), as well as the use of renewable heat is becoming increasingly important. The individual heat transfer stations, which form the link between district heat suppliers and end consumers, are of particular importance for an optimal district heating system. The following two points are essential for an efficient and economic supply:

- Control and operating strategies that exploit all optimization potentials, integrate favorable renewable heat sources and enable a high degree of utilization over year-round operating concepts.
- Development of a multifunctional heat transfer station which can be integrated into an optimized control strategy.

The development of bidirectional heat transfer stations in combination with intelligent control strategies for entire district heating systems is to be carried out in the course of the research project *MULTI-transfer* (Rabensteiner et al., 2017). The systems are studied both for new buildings as well as for the stock. A detailed consideration of two application cases on the secondary side is carried out:

- Solarthermics
- Waste heat integration by heat pumps (e.g. from refrigeration plants)

2. HYDRAULIC INTEGRATION

Measures on a single point in the grid (e.g. on the secondary side) can have effects on the entire grid. Therefore, the entire system has to be considered when a bidirectional heat transfer station is installed. The pressure in the district heating line is very important. Similar pressures on the primary and secondary side are advantageous. The integration of prosumers with certain infeed variants becomes more difficult at higher pressures in the primary circuit. The low flow in summer can lead to hydraulic problems when integrating prosumers. Today, there is almost no experience in the hydraulic design of such systems.

The integration of decentralized heat generators into the grid can be carried out directly, hydraulic separated by means of a heat exchanger or hydraulic decoupled via a hydraulic separator or with a decentralized energy storage. Prerequisites for a direct connection are that the

decentralized heat source can withstand the high-pressure level and that only water is used. A hydraulic separation is always required for the integration of solarthermics and refrigeration systems.

The location of the prosumer in the district heating system is important. The stabilization of the system pressure is of utmost importance and allows easier feeding into the district heating system. Especially in the case of pipes made of steel, the temperature in the system must also be kept as constant as possible to avoid fatigue fractures due to thermal stresses (Kim et al., 2016). The location can limit the infeed of prosumers in already existing systems. In individual cases, the water column may even come to a standstill, particularly in cases of prosumer installations nearby to strand ends. According to Streicher (2005) there are basically three technical possibilities when feeding heat into existing district heating systems (compare Fig. 1):

- Flow from the return to the forerun
- Return rise
- Forerun rise

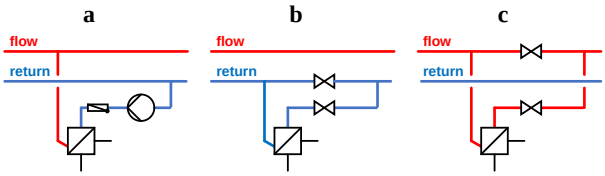

Fig. 1: *Hydraulic integration of decentralized heat suppliers: Flow from the return to the forerun (a), Return rise (b), Forerun rise (c)*

The abstraction of the heat transfer medium from the return line and the re-feed into the forerun line (Fig. 1a) requires a high pumping power because the differential pressure between forerun and return line has to be overcome. The small flow and the high differential pressure (up to 1 bar) could be problematic during infeed. There are only a limited number of pump manufacturers for such applications. The return temperature remains constant during infeed using this hydraulic integration variant.

The abstraction and re-feeding of the heat transfer medium takes place in the return line using the return rise (Fig. 1b). The pump energy is provided by the network pumps or by own heat exchanger pumps. A pressure-reducing valve must be provided in the return line in the first case in order to be able to control the flow through the heat exchanger. The heat exchanger pumps overcome the pressure losses of the heat exchanger, the control valve and the connecting lines. The efficiency of the centralized heat source is slightly reduced when a condensing boiler is used. Only additional energy can be introduced into the district heating system. The primary heat generator cannot be completely replaced. A return rise with the associated higher return temperatures is not advantageous in many smaller grids. However, a return rise can be quite useful in the case of relatively high temperature levels.

The heat transfer medium is abstracted from the forerun, passed through the bidirectional heat transfer station (heat exchanger) and fed back into the forerun, when using the forerun rise (Fig. 1c). As with the return rise, a pressure-reducing valve has to be installed into the district heating line – in this case, however, not in the return but in the forerun line. The pressure-reducing valve can be dispensed by installing a heat exchanger pump. The grid losses increase due to the higher grid temperature. The efficiency of the primary heat generator remains unchanged.

3. BIDIRECTIONAL HEAT TRANSFER STATION

Fig. 2 shows the hydraulic scheme of the bidirectional heat transfer station. This interconnection enables that heat can both be obtained from the grid and be fed into the grid by all three variants described above. 4 connection points are necessary at the district heating line. A speed-controlled pump is used on the primary side of the transfer station. Therefore, no pressure reducing valves are necessary in the corresponding district heating line. 4 and 2 three-way valves are installed on the primary and secondary side, respectively. By actuating these valves and switching on and off the corresponding pumps, various operating modes can be set. The associated interconnections can be seen in Fig. 3.

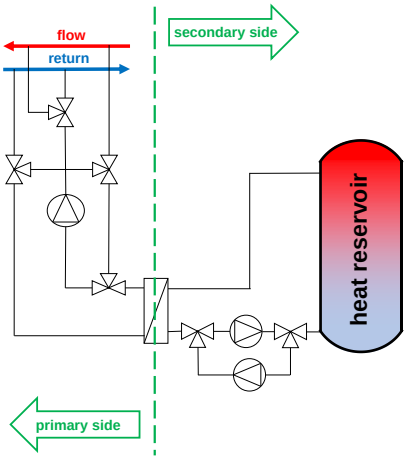

Fig. 2: *Hydraulic scheme of the bidirectional heat transfer station*

Initial cost calculations already show that this heat transfer station is a theoretical approach. The costs for the transfer station which allows all infeed variants are high. An installation is also complicated by the fact that 4 connection points on the district heating line are necessary. This means that additional lines are necessary at existing plants. The complexity is reduced for transfer stations that can only perform one infeed variant. Regardless of the chosen variant, however, at least 3 connection points are necessary, so that a new connection is inevitable for existing connections. The variant with the flow from the return to the forerun alone could preserve the two-line system.

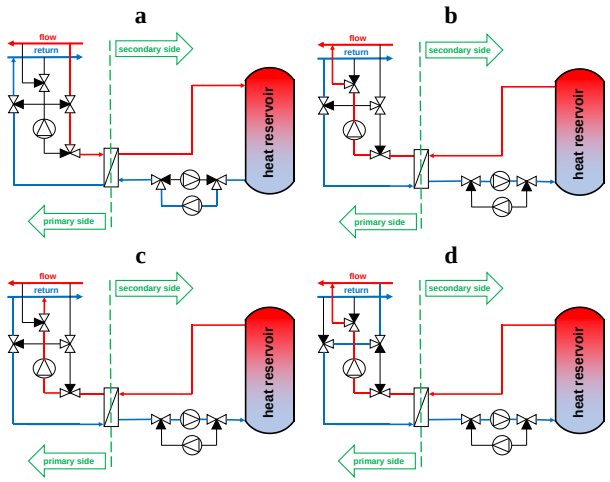

Fig. 3: *Switching of the bidirectional heat transfer station: Heat absorption from the grid (a), Flow from the return to the forerun (b), Return rise (c), Forerun rise (d)*

4. NUMERICAL MODEL

While in a laboratory test, the properties of a prosumer are examined, a numerical model is used to investigate the effects of several prosumer on the entire district heating system. The simulation model consists of two parts. The first model part depicts the primary side of the district heating system as detailed as possible, including the central heat source and the heat distribution system. Data from a real-life medium-sized district heating system is used as reference.

The second model (Fig. 4) forms the bidirectional heat transfer station and is individually set for each consumer/prosumer. The model considers stratified storages located at different consumers/prosumers. The model can be used to predict the time of heat input (into the district heating system) and the temperature level of this heat.

The illustrated simulation model in Fig. 4 calculates a prosumer with a solar thermal system. The model consists of different blocks. In the "Consumer" block, the data from the respective consumer of the reference district heating system are read in. Since a primary-side solar thermal system has already been installed at the heating plant on the reference district heating grid, real-time measured global radiation data can be acquired in the block "Solar data". The "Solarthermics" block calculates the available solar heat. The collector area was calculated according to the design diagram for solar collector surfaces for hot water preparation and heating support from Hoval GmbH. A solar coverage of about 25 % has been assumed. The size of the secondary storage was designed using the same diagram. The “Stratified storage” block calculates the

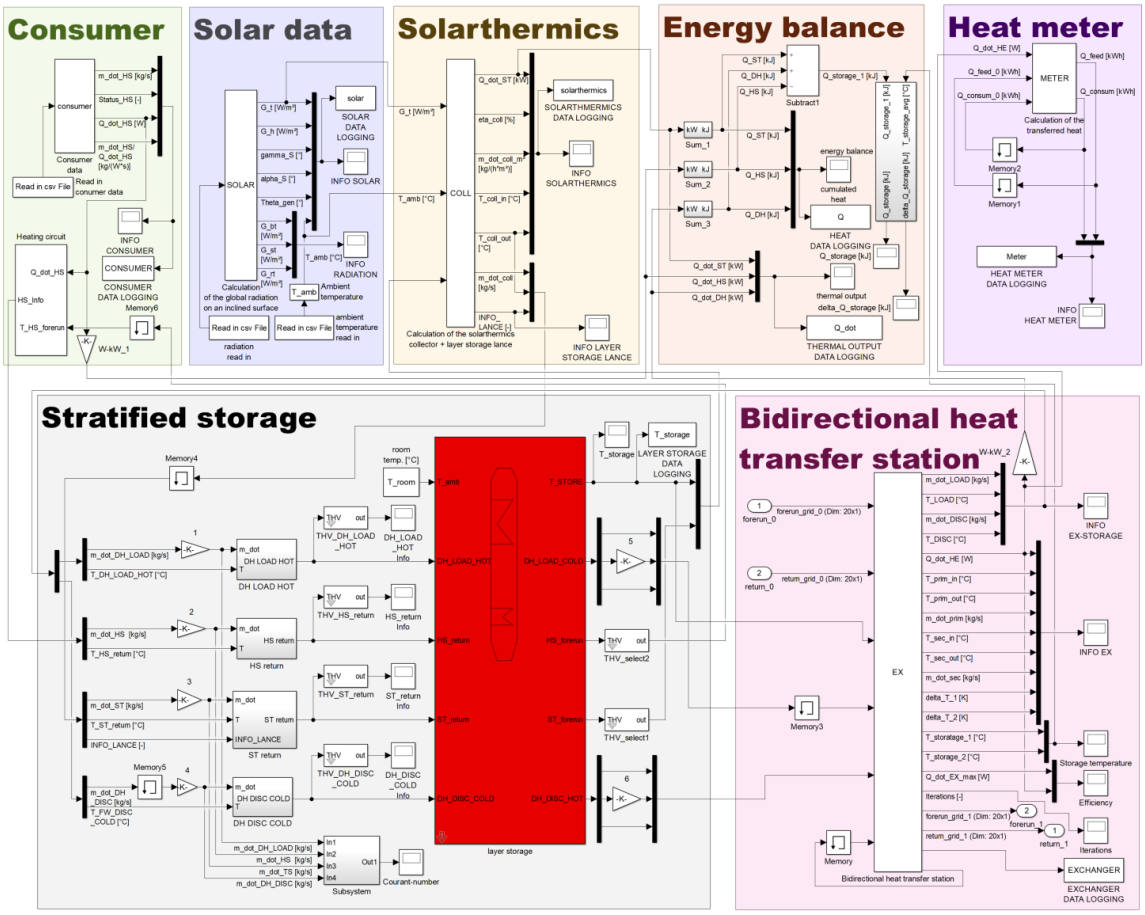

Fig. 4: *Simulation model of the bidirectional heat transfer station in Matlab/Simulink*

thermal stratification according to Eq. 1. The block called “Bidirectional heat transfer station” is the direct link between the grid and the prosumer and determines the operating mode based on the temperature in the storage and in the grid.

The two model parts allow an energetic and economical investigation of district heating systems with a large number of consumers/prosumers. This is enabled by combining the models. The primary side model receives data of the prosumers' strategy from the second model. Hydraulic problems such as flow reversals can also be investigated.

4.1 Control loops

The control loops of the simulation model are described with reference to Fig. 5. The heating circuit pump is controlled via the return temperature. A return temperature of 30 °C is assumed in the standard case. The heat output is taken from consumer data from the reference district heating system.

Three different operating options of the solar thermal system can be set. In the low-flow mode, the mass flow is 15 kg/(m²·h) in terms of the collector area. A mass flow of 40 kg/(m²·h) is set in the high-flow mode. In the matched-flow mode, the mass flow can vary between 1 and 50 kg/(m²·h). The mass flow is adjusted in 1 kg/(m²·h) steps in the just mentioned operation mode. The stratified storage is loaded via a stratified storage lance. Thereby, the return from the collector into the stratified storage can take place at different levels, but not at the same time. Normally, level 6 is fed. In the case of the matched-flow mode, the pump speed is controlled in such a way that the temperature of the feed medium corresponds to the storage temperature at level 6. If the mass flow rises above 50 kg/(m²·h), the inflow occurs one level higher (level 7). The higher temperature in the level above results in reducing pump speed and thus the volume flow is sinking. The infeed takes place up to level 11 with this control strategy. In the case of extreme solar irradiation, an injection at elevated temperatures can be carried out at the highest level. In the low- and high-flow mode, a stratified storage lance is also installed. The only difference between these variants is that the temperature cannot be adjusted to the respective level. This results in a slight disturbance in the thermal stratification.

The key factor as to whether the storage is charged or discharged is its temperature. The user can determine which temperature is to be used as the control variable for charging and discharging. The following selection options are available for the reference temperature:

- Average temperature in the storage
- Temperature of the lowest layer in the storage
- Temperature of the top layer in the storage

The corresponding three-way valves are activated, and the pump is switched on between heat exchanger and stratified storage if the reference temperature reaches a present value. During discharge, the corresponding reference temperature in the grid is used in addition to the reference temperature in the stratified storage. If the reference temperature in the stratified storage rises above a preset value, the storage temperature at level 11 is compared with the reference temperature in the grid. The reference temperature in the grid is the return temperature when using the return rise. Only when the highest storage

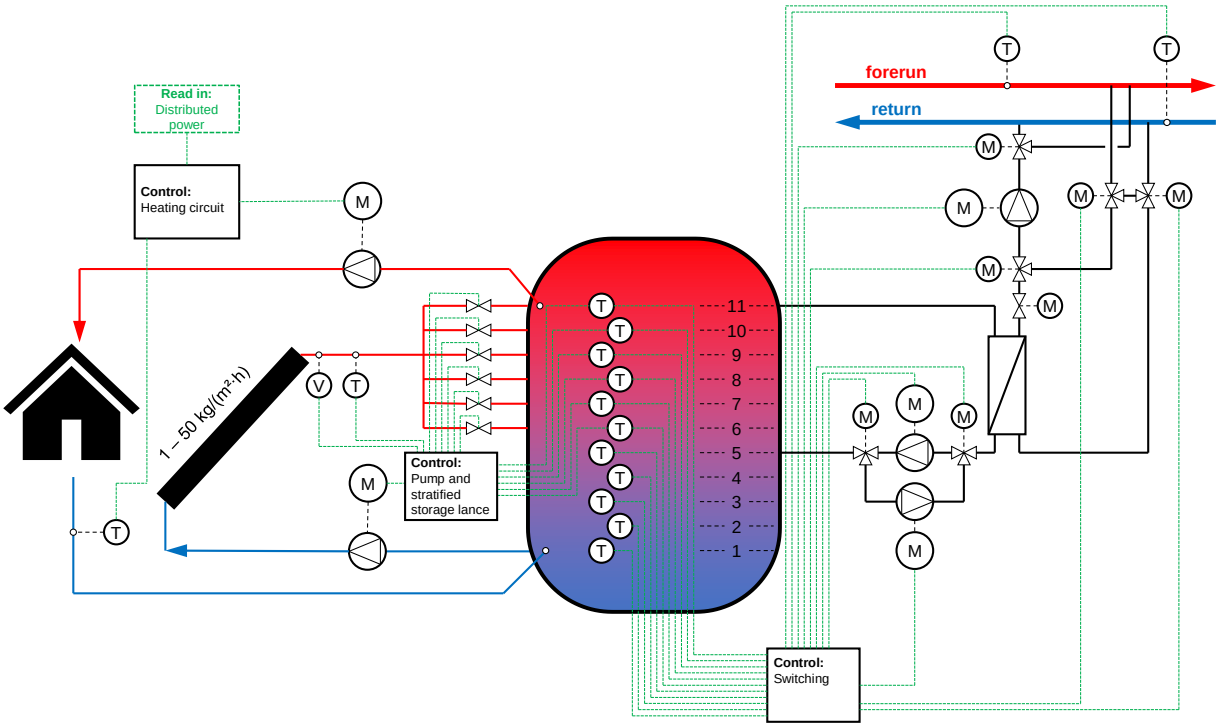

Fig. 5: *Control loops of the simulation model*

temperature (level 11) exceeds the return temperature in the grid, the heat flow from the prosumer towards the grid. For a possible infeed, the temperature in the uppermost layer of the storage must be significantly higher during the forerun rise. The forerun temperature of the grid is used as reference in this case. When using the infeed variant with the flow from the return to the forerun, the return temperature of the district heating line is also used as reference. In this case, indeed, it must be taken into account that, under certain circumstances, the resulting forerun temperature of the grid (after injection) decreases when the top storage temperature is lower than the forerun temperature of the grid (before feeding). However, there is nevertheless a heat flow from the prosumer to the grid, since this infeed variant increases the flow.

The loading of the storage occurs when the reference temperature in the storage falls below a pre-set value and the supply temperature in the grid is higher than the temperature in the uppermost layer of the stratified storage. For simulation purposes, a similar flow on the primary and secondary side is assumed. The maximum flow is determined either by the maximum flow rate of 2 m/s or by the maximum heat transfer capacity of the already installed heat transfer station of the individual consumers in the reference district heating system.

4.2 Influence of the reference temperature

For each of the following examples, a return rise as infeed variant is assumed. Charging and discharging takes place between 52 and 53 °C and 62 and 63 °C, respectively. The three examples differ only in the type of reference temperature. While in the first case, the average temperature in the storage is used, in the second and third case, the uppermost and the lowest temperature in the storage are used as reference.

Before describing the series of measurements, the mathematical model of thermal stratification will be explained briefly. The energy balance for each node of the stratified storage is calculated according to Eq. 1 (Solar-Institut Juelich, 1999).

$$\rho \cdot c_p \cdot \frac{dT_{node}}{dt} = \frac{(U \cdot A)_{loss}}{V_{node}} \cdot (T_{amb} - T_{node}) + \frac{\lambda_{eff}}{dh^2} \cdot \left(T_{node_{above}} + T_{node_{below}} - 2 \cdot T_{node}\right) + \frac{\dot{m}_{up} \cdot c_p}{V_{node}} \cdot \left(T_{node_{below}} - T_{node}\right) + \frac{\dot{m}_{down} \cdot c_p}{V_{node}} \cdot \left(T_{node_{above}} - T_{node}\right) + \frac{(U \cdot A)_{hx}}{V_{node}} \cdot (T_{hx} - T_{node}) \qquad \textit{Eq. 1}$$

The differences of the reference temperatures in the stratified storage and their effects on the operation of the bidirectional heat transfer station are listed below. Fig. 6 to Fig. 9 show the differences for a simulated day.

A thermal stratification is formed in the upper region of the storage when using the average storage temperature as reference (compare Fig. 6). There is no thermal stratification formation in the lower four levels. On the one hand, this is explained by the fact that charging and discharging via the grid takes only place between level 5 and 11.

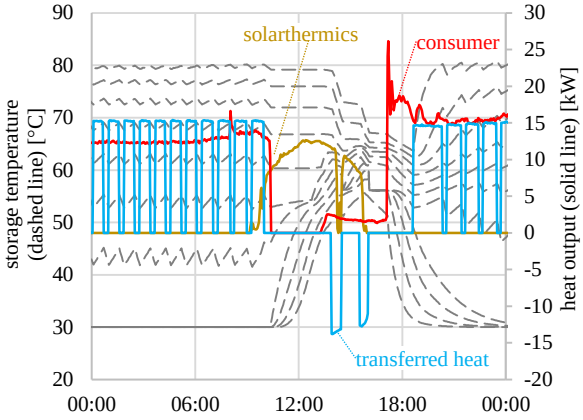

Fig. 6: *Storage temperature and heat output when using the average storage temperature as reference*

On the other hand, the mathematical model (Eq. 1) of the stratified storage simulation does not allow the consideration of temporal thermal stratification formation. During night and morning, the storage is periodically charged by the grid because of the constant heat transfer to the heating system (red line). A plus-sign in front of the transferred heat means that heat flows from the grid to the storage on the secondary side. Induced by solar yield, the average storage temperature rises, starting at about 10 am, so that no loading through the grid is required anymore. In addition, the heating system switches off immediately. The water is taken from the bottom layer during loading via the solar thermal system. A thermal stratification in the lower part of the storage is formed. The average storage temperature of 63 °C is exceeded at 2 pm. The transfer station switches to the infeed operation. When heat is feed into the district heating system, there is an increasing temperature drop with increasing storage height. The average storage temperature drops during discharging. After 35 minutes, the average storage temperature of 62 °C is already exceeded, resulting in termination of the discharge cycle. The short discharge cycle can be explained by the fact that discharging by heat transfer to the grid with 13.5 kW is considerably higher than the current solar yield (Shortly after 2 pm, there is a significant drop in the solar yield). A second discharge cycle starts at 3:30 pm. This leads to an increasing convergence of the lowest and highest storage temperature. In the evening, the solar yield drops back to zero and the heat absorption from the heating systems increases again. The average storage temperature decreases afterwards. A storage temperature of 52 °C is exceeded at about 6:30 pm and the storage has to be charged via the district heating grid. Due to the heating mode, return water with 30 °C reaches the lower part of the storage. Thus, the thermal stratification disappears again in this area.

Fig. 7 shows the system behavior when using the temperature of the uppermost layer as reference. The system is very sensitive. The charging cycles increase the temperature in the uppermost layer significantly, so that the reference value of 53 °C is reached quickly. Due to the short charging cycles, almost no thermal stratification occurs in the entire storage. The stratification arises only through the solar yield. In this variant, no discharge takes place via the grid for the day under investigation. After completion of the solar yield, the thermal stratification collapses again. The subsequent charging cycles are again very short. The storage capacity is only minimally used in this variant.

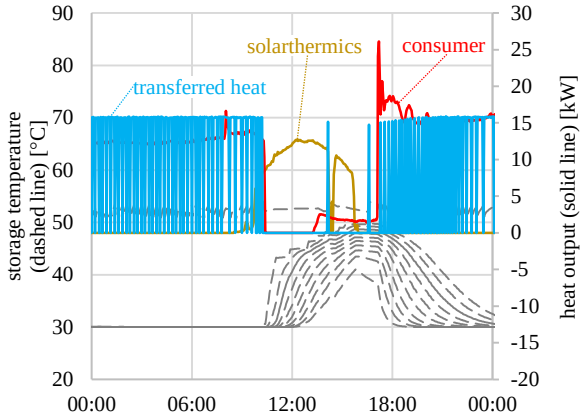

Fig. 7: *Storage temperature and transferred heat when using the temperature of the highest layer as reference*

Fig. 9 shows the system behavior when the temperature of the lowest layer in the stratified storage is used as reference. As it can be seen, the model can only adequately map this case. Since charging and discharging via the district heating system does not affect the lowest layer, the present reference temperature of the grid is the decisive factor for the operating state. The temperature in the uppermost layers corresponds approximately to the forerun temperature of the grid.

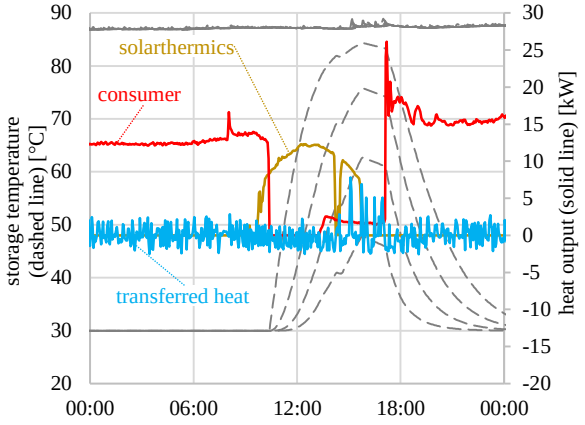

Fig. 9: *Storage temperature and heat output when using the temperature of the lowest layer as reference*

There is always a change from short charging and discharging cycles. Usually it should come to no discharge. Apparently, also short charging cycles occur when the flow temperature is below the temperature of the uppermost layer of the storage. Accordingly, it comes in a supposed charging cycle to a cursive discharge of the storage. Thus, in fact, a discharge of the storage occurs during a planned charging cycle.

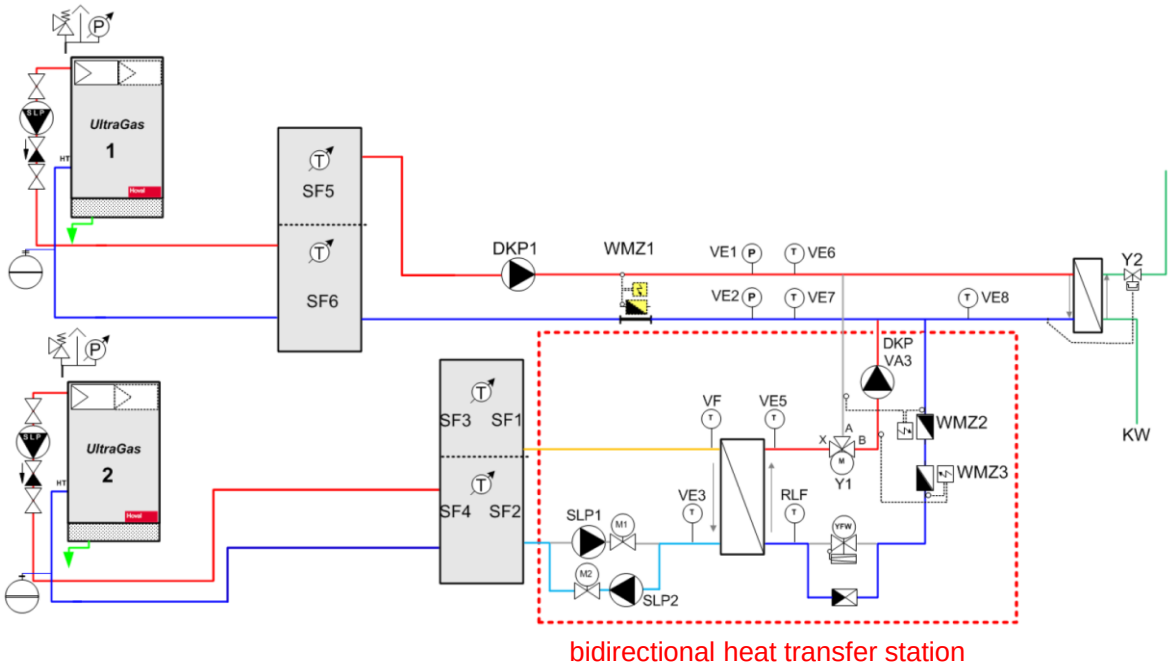

Fig. 8: *Laboratory test of the bidirectional heat transfer station*

4.3 Model validation by laboratory tests

The laboratory setup is shown schematically in Fig. 8. The central heat source of the district heating grid is simulated with a gas condensing boiler (UltraGas®, 50 kW). This boiler supplies a buffer tank. The pump DKP1 assumes the function of the network pump. Downstream consumers and prosumers are simulated by an adjustable heat exchanger. In addition to the heat absorption from the grid, the installed heat transfer station allows also an infeed by return rise. To overcome the pressure loss in the heat transfer station, the pump DKP VA3 is installed. Heat generation on the secondary side by the prosumer is also simulated by a gas condensing boiler (UltraGas®, 50 kW).

With regard to the simulation, the following changes occur for the laboratory operation:

- The loading of the stratified storage tank does not take place via a stratified storage lance.
- A discharge of the stratified storage tank can only take place via the grid. An extraction by the heating system was not included.

Fig. 10 shows the validation results for the plate heat exchanger. The dashed lines in this diagram and in the following indicate the measured values in the laboratory. The solid lines indicate simulation results.

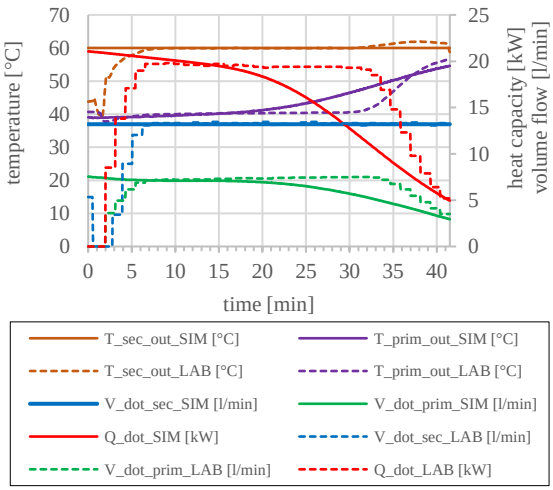

Fig. 10: *Validation of the heat transfer station (without consideration of inertia)*

The inertia of the system is not considered in Fig. 10. Effects of this neglection can be seen most clearly in the temperature difference of the secondary outlet temperature between simulation and laboratory in the first 5 minutes. While in the simulation over the entire loading cycle, the charge temperature is constantly 60 °C, the charge temperature in the laboratory test reaches this value only after 8 minutes. The reason for this behavior is the cooling of the line between heat transfer station and buffer storage. This neglection also leads to the fact that already at the beginning of the loading cycle, the transferred heat output has a maximum in the simulation. After that, the power drops. Unlike in the laboratory, the power decreases faster, so that in the study area, the amount of transferred heat is about the same size. Also in the simulation, there is a volume flow from the beginning on both the primary and secondary sides.

Taking into account the inertia of the heat transfer station, a line with a certain length was assumed between the transfer station and the secondary buffer. Thus, the cooling in the intermediate circuit could be well imitated (see Fig. 11 and Fig. 12).

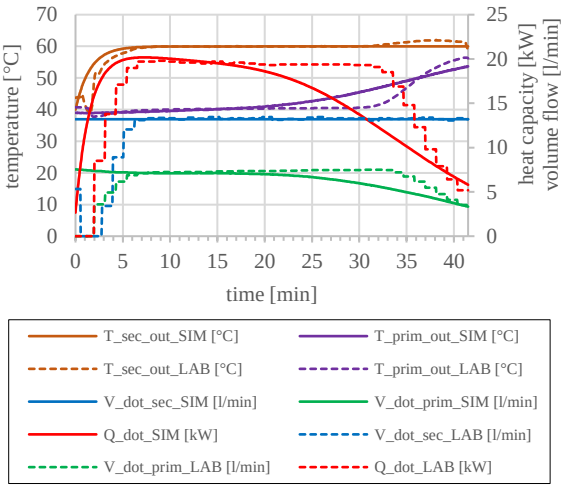

Fig. 11: *Validation of the heat transfer station (with consideration of inertia)*

For the comparison of the stratified storage temperatures in the buffer storage, the temperatures of the 11 nodes of the simulated stratified storage were used which are close to the installed temperature sensors. The uppermost storage temperature in the simulation fits very well with the measurement results, as shown in Fig. 12. With decreasing height, however, the deviation between simulation and measurement becomes larger. This can be explained by the fact that the transmitted heat output in the simulation is significantly higher in the first 5 minutes.

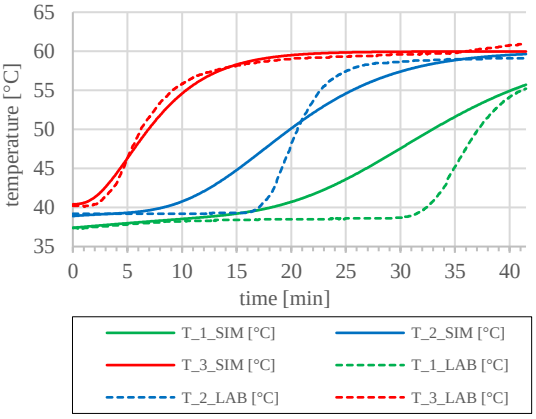

Fig. 12: *Validation of the buffer storage (with consideration of inertia)*

4.4 Simulation of strands

The installation of the model described above in certain areas of the district heating grid can endanger the security of supply of certain consumers and prosumers. Particularly in the area of strand ends, there is a potential danger for downstream consumers.

For example, when using the return rise, increased return temperatures may occur during infeed. This happens when the prosumer feeds and the downstream consumption is low at the same time. The risk of this scenario is particularly high, when solar thermal plants are installed on the prosumer sides. Due to the low demand of the downstream consumers/prosumers, the corresponding flow in the forerun and return line is low. A heat input by return rise has a huge impact on the return temperature. Prosumers which are located upstream on the same strand are confronted in this case with a very high return temperature, so that they can hardly feed-in at the same time with the same variant. In the case of forerun rise, however, the downstream prosumers are more affected through the high forerun temperature. An overall regulation of the consumers and prosumers in the line can solve this problem. In addition, a bypass at the heat transfer station of the last consumer in the strand can defuse this problem.

Problems may also arise during feed-in on strand ends by using the variant with the flow from the return to the forerun. This problem occurs when the prosumer is fed in and the temperature in the secondary storage is insufficient, thereby lowering the forerun temperature for the downstream consumers. Thus, under certain circumstances, the security of supply can no longer be guaranteed. Therefore, it is advisable to feed in only when the temperature of the uppermost layer in the stratified storage has exceeded the current flow temperature.

5. CONCLUSIONS

The numerical simulation of a bidirectional heat transfer station in Matlab/Simulink is explained in the present research work. The simulation model consists of two parts and takes into account both the primary side of the district heating grid and the secondary side with the decentralized heat source. The simulation model of the primary side was validated on the basis of measured data from the consumers, the boiler house and the grid points with the smallest differential pressure between forerun and return of a reference grid.

In a first sensitivity analysis, which is very important for the later validation by the laboratory measurements, the effects of different control parameters were described. It was shown that the average storage temperature is best used as a reference.

The validation of the simulation model of the bidirectional heat transfer station was carried out by means of laboratory tests. It turns out that the simulation model can reproduce the measurements relatively accurately. For faster load changes, however, the inertia of the system must be taken into account, which was carried out during the validation.

In the simulation of strands with several prosumers and consumers, problems have been raised that will be solvable by a cross-system control alone.

NOMENCLATURE

A_{loss}	Surface area for losses of one storage node	[m²]
λ_{eff}	Effective axial thermal conductivity	[W/(m·K)]
c_p	Heat capacity of fluid	[J/(kg·K)]
dh	Distance between two nodes	[m]
$\dot{m}_{down}$ $\dot{m}_{up}$	Vertical mass flow rate	[kg/s]
ρ	Density	[kg/m³]
T	Temperature	[K]
t	Time	[s]
U_{loss}	Heat loss coefficient	[W/(m²·K)]
V_{node}	Node volume	[m³]

REFERENCES

Averfalk, H., Werner, S., 2017. Essential improvements in future district heating grids. Energy Procedia 116, pp. 217-225

FGW, 2016. Zahlenspiegel – Erdgas und Fernwärme in Österreich. http://www.fernwaerme.at/media/uploads/misc/zahlenspiegel_2016.pdf

Kim, J., Kim, J., Cho, C., 2016. Experimental study for the reinforcement of district heating pipe. Transactions of the Korean Society of Mechanical Engineers A, Vol. 40, No. 3, pp. 245-252.

Lund, H., Möller, B., Mathiesen, B.V., Dyrelund, A., 2010. The role of district heating in future renewable energy systems, Energy 35, pp. 1381-1390.

Rabensteiner, M., Kraußler, A., Hummer, E., 2017. Simulation of bidirectional heat transfer stations in district heating grids. Book of abstracts: 3rd International Conference on Smart Energy Systems and 4th Generation District Heating.

Solar-Institut Juelich, 1999. CARNOT Blockset Version 1.0 – User´s Guide.

Streicher, W., 2005. Dezentrale Einspeisung von Erneuerbaren Energieträgern in Fernwärmenetze und Möglichkeiten der Biomasse KWK. Erneuerbare Energien für bestehende Fernwärmenetze, Graz, Austria, 20.04.2005.